CC Chemokine MIP-1β Can Function As a Monomer and Depends on Phe13 for Receptor Binding[†]

Jennifer S. Laurence,[‡] Cedric Blanpain,[§] John W. Burgner,[||] Marc Parmentier,[§] and Patricia J. LiWang*,[⊥]

Department of Biochemistry and Biophysics, Texas A&M University, College Station, Texas 77843-2128, Department of Chemistry, Purdue University, West Lafayette, Indiana 47907-1393, IRIBHN, Université Libre de Bruxelles, Campus Erasme, 808 route de Lennik, B-1070 Bruxelles, Belgium, and Department of Biological Sciences, Purdue University, West Lafayette, Indiana 47907

Received October 5, 1999; Revised Manuscript Received January 10, 2000

ABSTRACT: The reported structures of many CC chemokines show a conserved dimer interface along their N-terminal region, raising the possibility that the quaternary arrangement of these small immune proteins might influence their function. We have produced and analyzed several mutants of MIP-1β having a range of dimer K_d values in order to determine the significance of dimerization in receptor binding and cellular activation. NMR and analytical ultracentrifugation were used to analyze the oligomeric state of the mutants. Functional relevance was determined by receptor binding affinity and the ability to invoke intracellular calcium release from CHO cells transfected with the MIP-1β receptor CCR5. The monomeric N-terminally truncated mutant MIP(9) was able to bind the CCR5 receptor with a K_i of 600 pM but displayed weak agonistic properties, while the monomeric mutant P8A still retained the ability to tightly bind (K_i = 480 pM) and to activate (EC_{50} = 12 nM) the receptor. These data suggest that the MIP-1β dimer is not required for CCR5 binding or activation. In addition, we identified Phe13, the residue immediately following the conserved CC motif in MIP-1β, as a key determinant for binding to CCR5. Replacement of Phe13 by Tyr, Leu, Lys, and Ala showed the aromatic side chain to be important for both binding to CCR5 and chemokine dimerization.

Chemokines are small, secreted proteins involved in the recruitment and activation of lymphocytes and phagocytes during the inflammatory response. They have been implicated in the progression and modulation of a variety of immunological diseases such as arteriosclerosis, rheumatoid arthritis, and more recently AIDS (for reviews, see refs *2*−*6*). The chemokine superfamily includes more than 40 proteins, categorized into two major subfamilies (CC and CXC) and two minor subfamilies (CX_3C and C) based on their conserved N-terminal cysteine patterns (*3*).

High-resolution structures have been reported for several chemokines from the various subfamilies, revealing a conserved monomeric subunit fold for these proteins (*7*−*16*). The conserved Cys motif is preceded by a disordered N-terminal region of low sequence identity and is followed by a fold that is similar among chemokines, composed of three antiparallel β-strands and a C-terminal α-helix. In all cases studied, the N-terminal region of the chemokine is crucial for activity (*17*−*21*). Almost all chemokine structures reveal a dimer, although recently some monomers have been reported (*14*, *16*, *22*−*24*). Interestingly, the quaternary structure that has been observed shows a different pattern of self-association between the CC and CXC subfamilies. Dimerization of CC chemokines occurs along their N-termini such that this region becomes buried in an antiparallel β sheet. In contrast, the CXC chemokines interact via the β1 strand, placing the dimer interface on the other side of the structurally conserved β sheet from the N-terminus and leaving the N-terminal region highly solvent exposed.

The different dimer types observed for CC and CXC chemokines, along with the observation that the two subfamilies bind to completely different receptors, has led to the question of whether the dimer is a structurally important unit for chemokine action. Several experiments have addressed this question for the CXC chemokine IL-8,[1] which imply an active monomer for IL-8 (*25*), but do not rule out a role for the dimer (*26*). The question of dimer versus monomer is more complicated when considering the CC chemokines, because the dimer interface directly involves

[†] Funding was provided by the National Science Foundation, Grant MCB 9733907. M.P. was supported by the *Actions de Recherche Concertées* of the Communauté Française de Belgique, the French *Agence Nationale de Recherche sur le SIDA*, and the BIOMED and BIOTECH programs of the European Community (Grants BIO4-CT98-0543 and BMH4-CT98-2343). C.B. is Aspirant of the Belgian *Fonds National de la Recherche Scientifique*.

* To whom correspondence should be addressed. Phone: (409) 845-5616. Fax: (409) 845-9274. E-mail: pliwang@bioch.tamu.edu.

[‡] Department of Chemistry, Purdue University.

[§] Université Libre de Bruxelles.

[||] Department of Biological Sciences, Purdue University.

[⊥] Texas A&M University.

[1] Abbreviations: MIP-1β, macrophage inflammatory protein-1β; MIP-1α, macrophage inflammatory protein-1α; MCP, monocyte chemoattractant protein; RANTES, regulated on activation of normal T cell expressed and secreted; IL-8, interleukin-8; HIV, human immunodeficiency virus; CCR, CC chemokine receptor; CHO, chinese hamster ovary; WT, wild-type; NMR, nuclear magnetic resonance; HSQC, heteronuclear single quantum coherence; DSS, 2,2-dimethyl-2-silapentane-5-sulfonate, sodium salt; EDTA, ethylenediaminetetraacetic acid; ECL2, extracellular loop 2 (of the CCR5 receptor).

10.1021/bi9923196 CCC: $19.00
Published on Web 03/03/2000

the N-terminus, which is itself crucial for activity. Therefore, experiments that involve mutating dimer interface residues may affect function either because the dimer is important for receptor activation or because the mutated residues themselves are important for function. For instance, N-terminally truncated CC chemokines have been reported to have dramatically altered function, often acting as receptor antagonists (*17*, *19*, *20*). It is likely that many of these mutant chemokines are monomers (*1*), although it had not been determined whether the monomeric structure caused the loss of activity. While several dimer dissociation constants have been reported to be significantly higher than the nanomolar biological concentrations of these CC chemokines: 35 μM for RANTES (*15*) and 33 μM for MCP-1 (*27*), the MCP-1 dimer dissociation constant has been reported by others to be 500 nM (*28*). Since cross-linked MCP-1 dimers have been shown to be active, some have argued in favor of an active MCP-1 dimer (*29*). However, the MCP-1 monomer, made by the Pro8Ala mutation, possesses full activity on the receptor CCR2b (*28*).

While most data suggest a role for the chemokine monomer, the idea of dimerization or aggregation influencing function cannot be dismissed. Chemokines interact with glycosaminoglycans on the cell surface and these sugars have been reported to enhance local chemokine concentrations, which may increase the degree of multimerization (*30*). It has been reported that heparin causes aggregation of several types of chemokines and also that the presence of cell surface sugars is necessary for the full anti-HIV action of RANTES (*31*). Therefore, it is likely that the cell surface concentration of chemokines is significantly higher than that found circulating in the blood, making quaternary structure more relevant than the dimer dissociation constants obtained in solution might predict.

To assess the role of dimerization in binding and signaling, we generated several mutants of MIP-1β, which we predicted to lack the propensity to dimerize along the N-terminal interface. Nuclear magnetic resonance (NMR) and analytical ultracentrifugation were used to assess the dimer dissociation constant of each mutant, and then each mutant's ability to bind to and promote calcium release from CHO cells transfected with CCR5 was tested.

MATERIALS AND METHODS

Protein Production and Purification. The gene for MIP-1β was a gift from W. Leonard. The mutants were subcloned into the Novagen (Milwaukee, WI) pET-32-LIC/Xa or pET-21 plasmid according to the protocol from Novagen. However, alterations were made to pET-32-LIC (removal of the gene for the thioredoxin fusion peptide) to obtain a vector suitable for expression and purification of the proteins. Wild-type and all point mutants were expressed in the pET-32 vector and contained no N-terminal modification. The DNA for MIP(7) and MIP(8) were subcloned into pET-21d, which resulted in an N-terminal Met-Ala and a C-terminal His tag. MIP(9) was constructed with an N-terminal Met and both with and without a C-terminal His tag. The functional results obtained from the protein resulting from both MIP(9) constructs were identical. Electrospray mass spectrometry produced values consistent with the N-terminal Met having been removed from MIP(9). Point mutants were created using the QuikChange (Stratagene, La Jolla, CA) method, and all constructs were confirmed to be correct by DNA sequencing. The plasmids were transfected into BL21-(DE3) cells (Novagen) and the protein produced and purified as described previously (*1*), using a modified procedure from Kuna et al. to refold each mutant (*32*). Factor Xa (Novagen) was added to the appropriate samples, and proteolysis was allowed to proceed for several days. The digested fragments were separated using the C4 column and lyophilized. For NMR analysis, the lyophilized protein was taken up in 20 mM sodium phosphate buffer (pH 2.5) with or without the addition of 150 mM NaCl. In addition, 5% D_2O (Isotech, Miamisburg, OH) was added. For ^{15}N relaxation studies, the concentrations of protein of F13A and P8A were 0.6 and 1.0 mM, respectively. For analytical ultracentrifugation, the dry powder was taken up in 20 mM trifluoroacetate (pH 2.5) and 150 mM NaCl and dialyzed overnight in 3500 MW Slide-A-Lyzer Mini Dialysis Units (Pierce, Rockford, IL) against 2 L of the same buffer. Buffer was taken from the last 2 L solution and used in the reference cell in the centrifuge. Protein concentrations were calculated based on their UV absorbance at 280 nm, and sample purity was judged to be greater than 95% by SDS−PAGE, MALDI mass spectrometry, or both (data not shown). Each mutation produced a folded protein as judged by ^{15}N HSQC spectra (sample spectra shown in Figure 1).

Cell Culture. A CHO-K1 cell line coexpressing CCR5, $G_{\alpha16}$, and apoaequorin was described previously (*33*) and used for binding and functional assays. These cells were cultured using HAM's F12 medium supplemented with 10% fetal calf serum (Life Technologies), 100 units/mL penicillin, 100 μg/mL streptomycin (Life Technologies), 250 μg/mL Zeocin (Invitrogen, Carlsbad, CA), and 400 μg/mL G418 (Life Technologies).

[^{125}I]MIP-1β Binding Assays. CCR5 expressing CHO-K1 cells were collected from plates with Ca^{2+}- and Mg^{2+}-free PBS supplemented with 5 mM EDTA, gently pelleted for 2 min at 1000*g*, and resuspended in binding buffer (50 mM Hepes, pH 7.4, 1 mM $CaCl_2$, 5 mM $MgCl_2$, and 0.5% BSA). Competition binding assays were performed in Minisorb tubes (Nunc), using 0.08 nM [^{125}I]MIP-1β (2200 Ci/mmol, New England Nuclear, Cambridge, MA) as tracer, variable concentrations of competitors, and 40 000 cells in a final volume of 0.1 mL. The lyophilized chemokines were dissolved as 10 mM solutions in sterile phosphate-buffered saline (PBS) and stored at −20 °C in aliquots. They were diluted to the working concentrations immediately before use. Total binding was measured in the absence of competitor, and nonspecific binding was measured with a 100-fold excess of unlabeled MIP-1β. Samples were incubated for 90 min at 27 °C, then bound tracer was separated by filtration through GF/B filters presoaked in 1% BSA. Filters were counted in a β-scintillation counter. Binding parameters were determined with the PRISM software (Graphpad Software) using nonlinear regression applied to a single site competition model.

Calcium Release Assays. Functional response to chemokines was analyzed by measuring the luminescence of aequorin as described (*33*). CCR5, apoaequorin, and $G_{\alpha16}$ expressing cells were collected from plates with Ca^{2+}- and

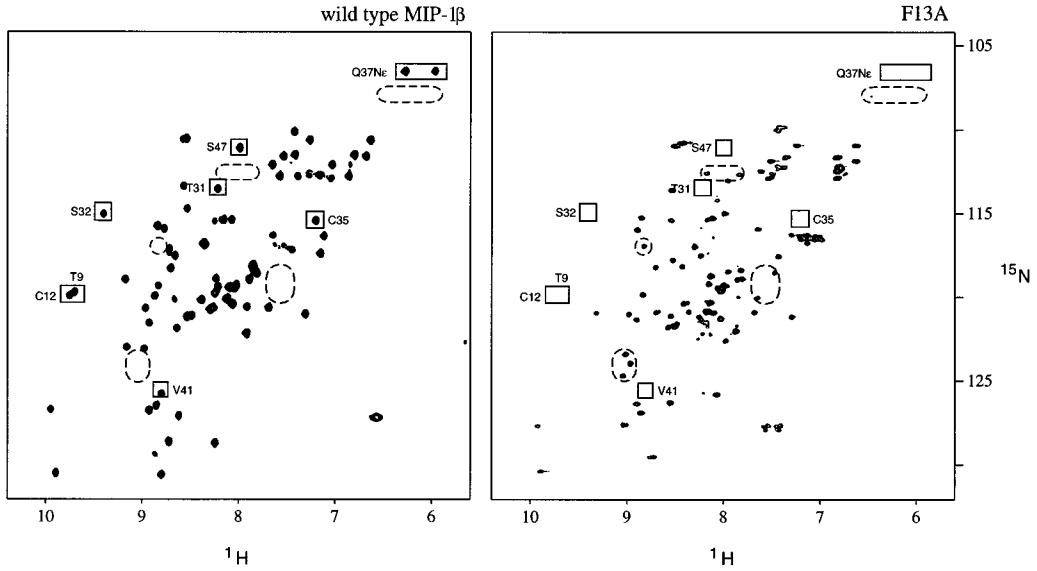

FIGURE 1: HSQC spectra of wild-type MIP-1β (A) and F13A (B) observed at pH 2.5, 20 mM sodium phosphate buffer. The concentration of wild-type MIP-1β was 800 μM and F13A was 1.2 mM. Peaks enclosed in solid boxes correspond to residues involved in dimerization that are sensitive to dissociation of the MIP-1β dimer. Peaks representing the monomeric form of the protein are encircled with dashed ovals.

Mg^{2+}-free DMEM supplemented with 5 mM EDTA, pelleted for 2 min at 1000*g*, resuspended in DMEM at a density of 5×10^6 cells/mL, and incubated for 2 h in the dark in the presence of 5 μM coelenterazine H (Molecular probes, Eugene, Oregon). Cells were diluted 7.5-fold before use. Agonists in a volume of 50 μL of DMEM were added to 50 μL of cell suspension (33 000 cells), and luminescence was measured for 1 min in a EG&G Berthold luminometer. For assaying antagonistic activities, chemokines were added to cell suspensions 1 min before measuring the functional response to 1 nM MIP-1β. EC_{50} values were determined with the PRISM software (Graphpad Software) using nonlinear regression.

NMR. NMR spectra were acquired at 25 °C on a Varian Unity Plus 600 MHz spectrometer equipped with a *z*-shielded gradient triple resonance probe, with the exception of the spectrum shown in Figure 1B, which was collected on a Varian Inova 500 MHz spectrometer equipped with an *xyz* gradient penta probe. HSQC spectra were collected with 512* points in the proton dimension and 128* points in the nitrogen dimension. A spectral width of 8000 Hz was used in the ^{1}H dimension and 1700.68 Hz for ^{15}N (for Figure 1B, 6000 Hz for ^{1}H and 1600 Hz for ^{15}N). The samples were placed in Shigemi tubes (Allison Park, PA) and the spectra referenced relative to DSS (*34*). T_1/T_2 ratios were determined using pulse sequences previously described by Tjandra et al. (*35*) and Farrow et al. (*36*) with ^{15}N delays of 21, 121, 301, 501, 761, 1001, and 1251 ms for the T_1 experiment and 32, 48, 72, 80, 96, 144, 160, and 192 ms for the T_2. An additional T_1 data point at 601 ms was collected for P8A. Sixteen scans were taken for each time delay, with 128 increments in the second dimension. NOE data were collected with and without a 3 s ^{1}H presaturation period, and a delay of 5 s was incorporated between scans. Thirty-two scans were acquired with 160 increments in the ^{15}N dimension. Each experiment was collected in randomized order and in an interleaved fashion to minimize experimental error due to spectrometer drift. The data were processed using the programs nmrPipe (*37*) and seriesTab (F. Delaglio, unpublished results). The reported T_1/T_2 ratios include only those residues having an NOE intensity of $\geq$0.6. Peaks from the WT spectra were identified based on the high-resolution NMR structure of MIP-1β (*11*).

NMR was also used to track the dissociation of the MIP-1β dimer over a range of protein concentrations. The following peaks were found to both change position in the transition from the dimer to the monomer and to be easily identifiable on the HSQC spectra: T9, C12, T31, S32, C35, S47, V41, and Q37 Nϵ. These peak heights in the dimer spectra could be compared to the peak heights of resonances that had shifted due to dimer dissociation. We compared the values calculated from the sedimentation equilibrium data for mutants F13Y and F13L to a series of HSQC spectra acquired at various protein concentrations to determine the viability of this method. From this analysis, it became clear that we could use relative peak intensities to approximate K_d values that fall in the micromolar range with a reasonable amount of certainty. While the exchange rate of the amides could differ between the two states and produce peak intensities that cannot quantitatively be compared, amide exchange rates are minimal at the low pH at which we measure the spectra. The values for mutants L34A and T9D and for the N-terminally truncated mutants MIP(7) and MIP-(8) were estimated in this manner, while the K_d of all other mutants reported were rigorously determined, either by analytical ultracentrifugation or by ^{15}N NMR relaxation measurements.

Analytical Ultracentrifugation. Sedimentation equilibria data were collected on a Beckmann XL-A analytical ultracentrifuge. Data were collected at 25 °C and 25 000, 30 000, and 42 000 rpm. The protein concentrations used were 330 nM, 1 μM, and 10 μM for MIP-1β; 10 and 67 μM for F13Y; and 1, 10, and 155 μM for F13L. Samples were monitored at 280 nm for concentrations of $\geq$10 μM and at 220 nm for 330 nM, 1 μM, and 10 μM protein concentrations. These data were fitted to eq 1 by nonlinear progression analysis using the program Winnonln, which was obtained from the National Analytical Centrifugation Facility and is useful for

Table 1: Dimer K_d, EC_{50}, and K_i Values for MIP-1β and Mutants

	dimer K_d (μM)[e]	EC_{50} (nM)[e]	K_i (nM)
MIP-1β	0.73[a]	4.0 ± 1.5	0.39 ± 0.12
P8A	monomer[b]	12.0 ± 6.7	0.48 ± 0.18
T9D	30[c]	250 ± 150	54 ± 35
L34A	10[c]	4.7 ± 0.6	0.38 ± 0.10
F13Y	43[a,c]	6.8 ± 3.6	0.46 ± 0.07
F13L	133[a,c]	670 ± 460	77 ± 42
F13K	monomer[a,c]	480	290 ± 170
F13A	monomer[b]	>1000	>1000
MIP(7)	200[c]	760 ± 40	ND
MIP(8)	200[c]	480	ND
MIP(9)	monomer[b]	74 ± 7[d]	0.60

[a] Dimer K_d determined by analytical ultracentrifugation. [b] Dimer K_d determined by NMR relaxation experiments. [c] Dimer K_d estimated based on HSQC spectra. [d] All truncation mutants tested showed very little calcium release compared to the wild type protein, particularly MIP(9), which showed almost no calcium release. The EC_{50} for this mutant merely indicates the concentration of chemokine for which half of (very little) calcium release was measured. [e] Column 2 shows the EC_{50} for calcium release and column 3 shows the K_i, where lower numbers indicate higher affinity for CCR5. ND = not determined.

both detecting multiple equilibria and estimating the value of the equilibrium constants from the absorbance data. The total absorbance (A_t) for a monomer−dimer system at any distance (r) from the center of the rotor is defined by the equation

$$A_t = \delta A + A_m(r) + A_d(r) = \delta A + A_m(r) + K_2 A_m(r)^2 \quad (1)$$

where

$$A_m(r) = A_{m,0} \exp[\sigma(r^2 - r_0^2)/2 - 2B\sum(A_t - \delta A)] \quad (2)$$

$A_m(r)$, $A_d(r)$, and $A_{m,0}$ represent the monomer and dimer absorbance at any point in the cell and the smallest value of r, respectively. K_2 is defined by A_d/A_m. B indicates whether the macromolecule deviates from ideality. The reduced molecular weight (σ) is related to the true molecular weight of the monomer (M_p) by the equation

$$\sigma = M(1 - \upsilon_{bar}\rho)\omega^2/RT \quad (3)$$

in which υ_{bar} represents the partial specific volume of the protein and ρ the solvent density. The partial specific volume of the solute was calculated from the amino acid composition and the known volume (determined from the structure) divided by the molecular weight, which was adjusted for the ubiquitous presence of the heavy isotope ^{15}N. The other parameters were determined using the program Sednterp (obtained from the Boston Biomedical Research Institute RASMB web site) such that the theoretical values for σ determined for the monomer at 25K, 30K, and 42K rpm were 0.583, 0.839, and 1.64, respectively. Data sets were composed of experiments run at all three speeds and multiple concentrations for each protein in an appropriate concentration range. The data were processed using the program Winnonln using successive iterations to ensure that the data collected at various speeds and concentrations converged to a common value for ln K_2. Since the parameter having the most significant impact on the resulting K_d was $A_{m,0}$, the values determined from the 42 000 rpm runs for this variable were used in the global fit for each protein. Values for the global fits are reported in Table 1. After complete analysis, the simplest equation to which the data fit was the monomer−dimer equilibrium model for WT, F13Y, and F13L. The dimer K_d values were calculated from the ln K_2 determined by Winnonln using a molar extinction coefficient of 1.23×10^5/M, which was determined from the amino acid composition using the program Sednterp.

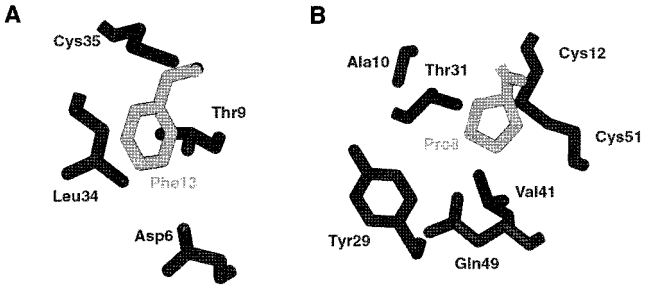

FIGURE 2: (A) The interactions made by residue Phe13 (light) with amino acids of the other subunit (dark) in the MIP-1β dimer. If any part of the side chain of Phe13 is within 5 Å of any part of the side chain of the amino acid of the other subunit, the entire amino acid side chain is shown. (B) The interactions made by residue Pro8 (light) with amino acids of the other subunit (dark) in the MIP-1β dimer. If any part of the side chain of Pro8 is within 5 Å of any part of the side chain of the amino acid of the other subunit, the entire amino acid side chain is shown. Data taken from reference ref *11*.

RESULTS

NMR is a useful technique to both quantitatively and qualitatively determine the oligomeric state of MIP-1β. The HSQC spectrum of wild-type MIP-1β (Figure 1A) contains peaks for Thr9 and Cys12 that resonate above 9.5 ppm as a result of their involvement in the chemokine dimer interface (Figure 2). We have shown that if the protein is mutated to favor dimer dissociation, these (and other) peaks no longer appear in the same region of the spectrum, while new peaks are visible, making it straightforward to identify the presence of monomer or dimer in the protein sample (*1*). All spectra reported here were collected at pH 2.5, due to the formation by MIP-1β of large aggregates above pH 3.5 that cannot be observed by NMR (*11*). Despite the unusually acidic conditions under which MIP-1β must be structurally analyzed, data from other CC chemokines show that the dimer is retained at higher pH (*10*). Indeed, it has been found for RANTES that the dimer is tighter at higher pH values (*15*), indicating that for our work with MIP-1β we may be underestimating the dimer affinity. This pH sensitivity affects several members of the subfamily (*38*−*40*).

We have shown by NMR a gradual decrease in the ability of MIP-1β to dimerize as more residues were removed from its N-terminus (*1*). This can be explained by the loss of several important intersubunit contacts, as increasing portions of the N-terminus were removed. The truncated mutants are named MIP (#), in which # indicates the residue number at the mutant's N-terminus. The truncated analogues MIP(7), MIP(8), and MIP(9) were tested for their ability to induce intracellular calcium release via CCR5. The results were generally consistent with the data published for other CC chemokines (*17*, *19*), showing a decrease in receptor activity with N-terminal truncations (see Table 1). However, the results of the binding assays show only a small difference in the ability of the severely truncated analogue, MIP(9), to

interact with the receptor compared to the wild-type protein (see Table 1). The wild-type MIP-1β binds to CCR5 with a K_i of 390 pM, and MIP(9) binds with a K_i of 600 pM. Therefore, our data indicate that large deletions at the N-terminus produce weaker agonists until MIP(9), which appears as a very weak agonist. To determine whether this loss of activity is due to composition or quaternary structure, we set out to design other mutants in addition to N-terminal truncation mutants that may be monomeric.

Analysis of the MIP-1β structure revealed several possible sites for disrupting the association without deleting the N-terminus, based on the number of close intersubunit contacts observed. The aromatic ring of Phe13 from one monomer closely interacts with the side chains of Leu34 and Thr9 from the other (Figure 2A). Accordingly, Phe13 and Leu34 were separately mutated to Ala. Thr9 was mutated to Asp, both because the ninth position is near the center of the hydrophobic dimer interface, making Asp likely to be quite disruptive due to its charge, and also because the very similar chemokine vMIP-II has an Asp at this position and has been shown to be monomeric (*22*). In an additional attempt to form a monomer, it was observed that Pro8 makes numerous interactions across the dimer (Figure 2B), so that residue was mutated to Ala.

Replacing Phe13 with Ala resulted in a completely monomeric protein, as shown by ^{15}N T_1 and T_2 relaxation analysis, which yielded a T_1/T_2 ratio of 3.92 $\pm$ 0.8 (data not shown). The average ^{15}N T_1 value, $\langle T_1 \rangle$, was 460 $\pm$ 39 ms, and the average ^{15}N T_2 value, $\langle T_2 \rangle$, was 122 $\pm$ 23 ms. The 28 residues used to calculate the $\langle T_1/T_2 \rangle$ were selected based on having NOE values above 0.6, to minimize the contribution of residues experiencing slow internal motion. The P8A mutation also successfully disrupted the dimer interface of MIP-1β, resulting in a monomeric protein, yielding an average T_1/T_2 ratio of 4.0 $\pm$ 0.45 for peaks with an NOE intensity of $\geq$0.6 (data not shown). Twenty-three residues were used to calculate the $\langle T_1/T_2 \rangle$. The $\langle T_1 \rangle$ was 455 $\pm$ 37 ms, and the $\langle T_2 \rangle$ was 115 $\pm$ 18 ms.

Relaxation analysis is a well-established way to determine the overall size of a protein or complex (*36*, *41*) and is particularly useful in determining the chemokine oligomeric state (*1*, *22*). The T_1/T_2 ratios found for F13A and P8A are quite similar to that found for the monomeric truncated mutant MIP(9) [3.1 $\pm$ 0.3 (*1*)] and to that for the monomeric chemokine vMIP-II [3.2 $\pm$ 0.3 (*22*)]. In contrast, wild-type MIP-1β has an average ^{15}N T_1/T_2 ratio of 8.3 and a correlation time of 8.6 ns, fully consistent with a protein dimer (*1*). On a more qualitative level, the F13A mutant yields an HSQC spectrum typical of a monomeric MIP-1β, lacking the distinctive Thr9/Cys12 peaks at 9.7 ppm, and showing the expected additional peaks encircled by dashed ovals in Figure 1B.

While the F13A mutant is clearly a monomer even at high concentration, the mutation of Leu34 and Thr9, both of which interact with Phe13 in the dimer, did not affect dimer affinity to such a large extent. The L34A mutation resulted in a protein with a dimer K_d near 10 μM as judged by observation of the HSQC spectra under various conditions, while the T9D mutation produced a protein with a dimer dissociation constant estimated to be 30 μM.

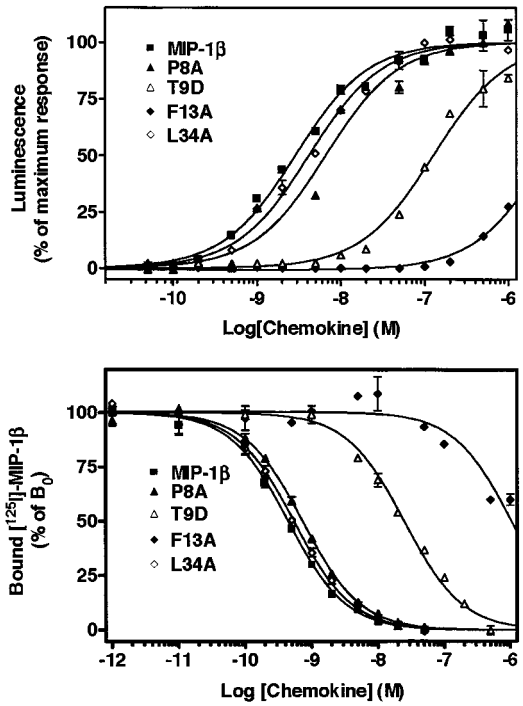

FIGURE 3: Graphs of CCR5 activity (A) and binding (B) for MIP-1β and several mutants that affect dimerization. Data has been normalized so that it is displayed as a percent of maximum luminescence (A) or binding (B) versus the amount of chemokine added for each species.

The activity of these dimer interface mutants on the sole known MIP-1β receptor, CCR5, is shown in Figure 3A, where productive receptor interaction is determined by measuring release of intracellular calcium stores. While the monomer F13A shows almost no activity on the receptor, the monomer P8A has an EC_{50} of 12 nM, a value that is only moderately reduced from the EC_{50} of 4.0 nM for the wild-type protein. The L34A mutation that did not greatly disrupt the dimer results in a protein that shows an activity similar to that of the wild-type protein, with an EC_{50} of 4.7 nM. The T9D mutation resulted in an EC_{50} of 250 nM.

The binding constant of each of these point mutants is largely consistent with their ability to promote calcium release (Figure 3B and Table 1). The monomer F13A binds CCR5 poorly, having a micromolar or worse K_i, whereas the monomer P8A has an average K_i of 480 pM. The slightly disrupted dimer L34A binds the CCR5 receptor with a K_i of 380 pM, while the T9D mutant binds quite poorly in comparison at 54 nM.

As the F13A mutation abrogated MIP-1β activity on the CCR5 receptor, Phe13 was also changed to Tyr, Leu, or Lys to determine which properties of this residue might influence receptor interaction. The NMR spectra for these mutants reveal that any change at this position reduces the inherent potential of the dimer interface to form, as evidenced by the presence of peaks indicative of the monomeric species (Figure 4). The effects seen in the HSQC spectra were confirmed to be the result of monomer−dimer equilibrium by sedimentation equilibria experiments in the analytical ultracentrifuge. From the ultracentrifuge data, the average dimer dissociation constants were calculated to be 730 $\pm$ 300 nM for MIP-1β, 43 $\pm$ 9 μM for F13Y, and 133 $\pm$ 31 μM for F13L (see Figure 5 and Table 1). In addition, the

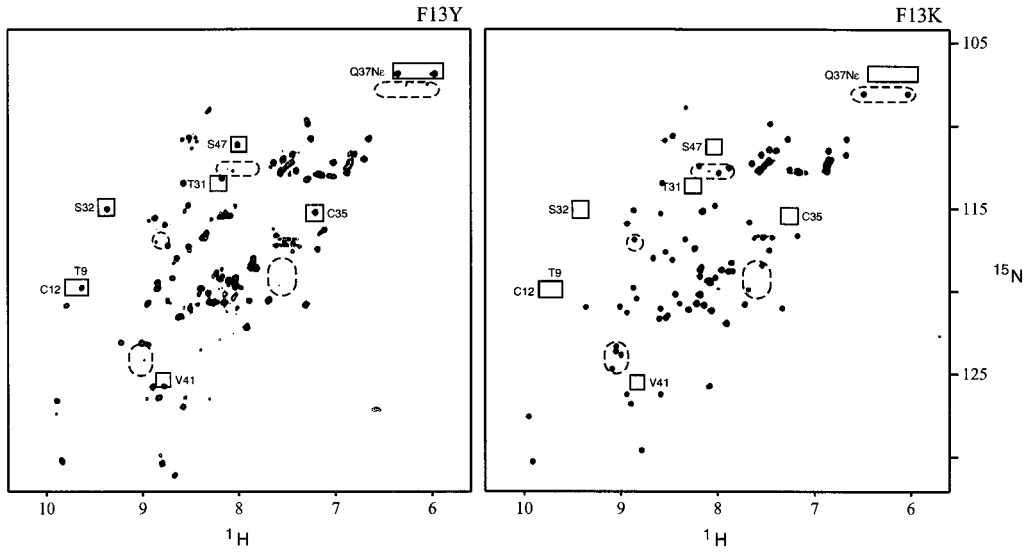

FIGURE 4: HSQC spectra of 300 μM F13Y (A) and 600 μM F13K (B) in 20 mM sodium phosphate, pH 2.5 and 150 mM NaCl. Peaks enclosed in solid boxes correspond to residues involved in dimerization that are sensitive to dissociation of the MIP-1β dimer. Peaks representing the monomeric form of the protein are encircled with dashed ovals.

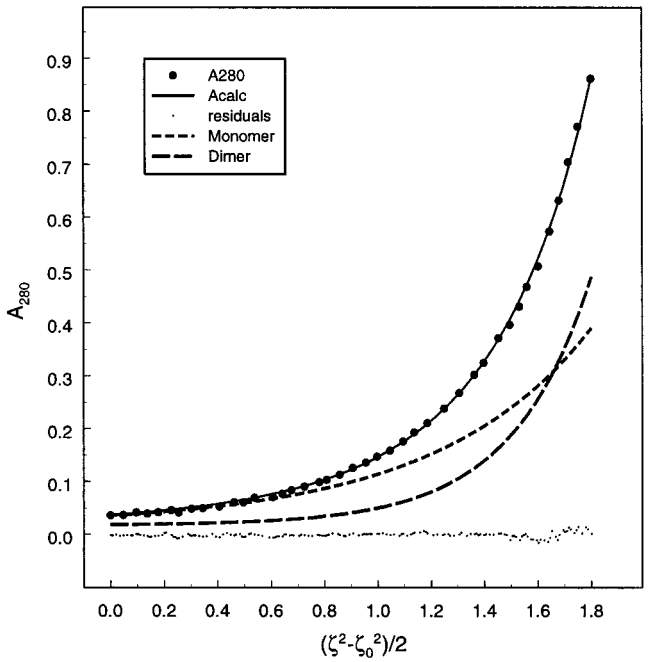

FIGURE 5: Analytical ultracentrifugation. The data in the plot correspond to the 42 000 rpm scan taken of 67 μM F13Y. The raw data points have been plotted to display the absorbance (A_{280}) of MIP-1β in solution versus position in the cell at equilibrium, referenced to the first data point [ζ,ζ_0 are the values for $r^2/2$ at position r in the cell and the reference position (first data point)]. The solid line indicates the calculated distribution for the theoretical total absorbance (A_{calc}) of the protein and the dashed lines represent the amounts of monomer and dimer found in solution at equilibrium. The residuals illustrate how well the data fit the monomer−dimer model as indicated by the small, random dispersion of the data about zero.

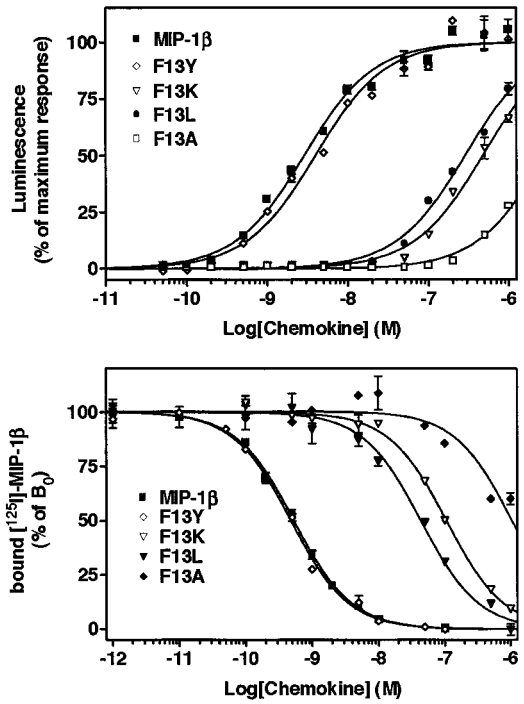

FIGURE 6: Graphs of CCR5 activity (A) and binding (B) for MIP-1β and the Phe13 mutants. Data has been normalized so that it is displayed as a percent of maximum luminescence (A) or binding (B) versus the amount of chemokine added for each species.

F13K data fit a single species analysis best, confirming that it does not form a dimer, even at 150 μM protein concentration.

The Phe13 mutants showed a wide range of activity on the CCR5 receptor (Figure 6A). Interestingly, the relative ability of these mutants to dimerize qualitatively corresponds to their relative ability to bind and activate the CCR5 receptor. As noted above, the monomeric F13A mutation shows almost no detectable ability to activate the CCR5 receptor, largely due to its inability to bind the receptor. At the opposite end of the range, the conservative mutation F13Y shows a clear ability to dimerize (although its dimer affinity is 60-fold lower than that of the wild-type protein). This mutation binds and activates the CCR5 receptor at near wild-type levels, having a K_i of 460 pM and an EC_{50} of 6.8 nM (Figure 6, Table 1). The F13L mutation results in a substantially weaker dimer, and the CCR5 binding and activation ability of this mutant is quite reduced (Figure 6B), with an inhibition constant of 77 nM and EC_{50} of 670 nM. Finally, the F13K mutation produced a monomeric protein as judged by its HSQC and analytical ultracentrifuge data.

This mutant's ability to bind and activate the receptor is correspondingly worse, with a competition binding constant of 290 nM and an EC_{50} of 480 nM for CCR5 activation (Figure 6).

DISCUSSION

Dimer Mutants. In an effort to determine the relevance of the MIP-1β dimer to its activity, we tested several mutants of MIP-1β having varying ability to dimerize. The data show that removing the N-terminus of MIP-1β drastically reduces both the ability of the mutant to dimerize and the activity of the mutant on the receptor CCR5. This may indicate the importance of dimerization on activity or it may be explained by the "two-site model" (*18*, *42*). In this model, the N-terminal amino acids of the chemokine are necessary for activity, while the N-loop amino acids (residues 12−20) are necessary for binding (*43*−*45*). The dimerization state of the chemokine is not important in the two-site model.

Despite the lack of receptor activation, the tight binding of MIP(9) shows that a monomer is sufficient for receptor binding to occur. To ascertain whether the MIP-1β dimer is important for receptor activation, mutants were designed such that the N-terminus of the protein would be largely intact, but the chemokine dimer would be disrupted. We were successful in disrupting the MIP-1β dimer with several of our mutations. F13A and P8A are completely monomeric at high concentrations, while L34A has a mildly reduced propensity to dimerize.[2] T9D still retains a fairly tight dimer under the low pH conditions of our structural assays, although we believe the dimer affinity of this mutant would be significantly reduced under physiological conditions where the Asp would be expected to be charged.

This set of mutants displayed a great disparity in their ability to interact with CCR5 but these differences did not necessarily correlate to the ability of the chemokine mutants to dimerize. The L34A mutation produced a moderately disrupted dimer, yet showed no detectable loss in binding compared to the wild-type protein, and its ability to activate the receptor was lowered by only 1.2-fold. The P8A mutant is fully monomeric even at high concentrations, yet showed only a moderate loss of activity: it requires 3-fold more P8A than the wild-type protein to reach 50% of maximum signal, while the receptor binding ability of P8A is only reduced by 19%. The F13A mutant shows the most dramatic effect on receptor interaction. This wholly monomeric mutant is almost completely unable to bind CCR5 with a correspondingly poor ability to cause receptor activation (see Figure 3 and Table 1). The T9D mutant shows significantly reduced ability to bind and activate the receptor (a reduction in activity by 63-fold and a reduction in binding by 140-fold), although the loss of activity is not as great as for the F13A mutant (Table 1, Figure 3). This effect is difficult to interpret structurally, however, because the ionization state of the Asp9 is likely different between the necessary conditions for NMR structural studies and the functional studies. Overall, the large difference in dimer affinity observed between wild-type MIP-1β, L34A, and P8A, all of which are quite competent in both binding and activating CCR5, also suggests that MIP-1β interacts with CCR5 as a monomer, producing little direct evidence to suggest a correlation between dimerization and CCR5 activity. As previously noted, MIP-1β is soluble only under acidic conditions at the concentrations required for determination of dimer dissociation constant, while receptor assays were carried out under standard conditions of low protein concentration and physiological pH. This does lead to the possibility that the dimer K_d values determined do not reflect the dimer K_d under the conditions of the activity assays. However, all of our mutants except T9D involve a nonionizing amino acid designed to break up largely hydrophobic interactions, so we believe that the dimer K_d values are qualitatively correct even at physiological conditions. Recently, mutants of several CC chemokines were reported that disrupt aggregation and may be useful in future studies (*46*).

Our results with these dimerization mutants of MIP-1β are largely consistent with work on other chemokines. Truncation mutants of both RANTES and MCP-1 have been shown to retain tight binding to their respective receptors (*17*, *19*). Similarly, an alanine replacement for an aromatic residue in the N-loop of both these proteins (F12A in RANTES and Y13A in MCP-1) showed a significant loss of binding to the chemokine receptor (*20*, *28*), with the most pronounced effect being the 5000-fold decrease in the ability of RANTES to bind CCR5. Finally, in a careful analysis of several structural mutants of MCP-1, Paavola et al. have recently concluded that MCP-1 likely binds the receptor CCR2b as a monomer (*28*).

Phe13 Mutants. Because the F13A mutation produces such a dramatic disruption in the ability of the protein to bind the CCR5 receptor, this amino acid seems to be important in receptor contact. To assess the impact of F13 on function, we made a series of mutations, including a conservative aromatic substitution (F13Y), a large hydrophobic substitution (F13L), and a charged amino acid replacement (F13K). Qualitatively for the Phe13 mutants, we find the same trend in ability to dimerize as in ability to activate or to bind the CCR5 receptor: for dimer affinity, WT > F13Y > F13L > F13K ≥ F13A; and for CCR5 binding, WT ≥ F13Y > F13L > F13K > F13A. Despite this interesting correlation, the order of magnitude of these effects is not equivalent. For instance, the F13Y dimer affinity is 60 times worse than the wild-type dimer affinity, yet the binding affinity for CCR5 is barely distinguishable, 460 ± 70 pM for F13Y and 390 ± 120 pM for the wild-type.

Our functional data collected on the Phe13 mutants suggest that the ability of MIP-1β to bind CCR5 depends heavily on the side chain located at position 13 (Figure 6). If the aromatic character is retained, as with the F13Y mutation, binding is consistent with that of wild-type and function is diminished by only a small amount. However, when an aliphatic group occupies this space, as with F13L, receptor binding decreases by greater than 2 orders of magnitude, and activity decreases proportionally. Changing to a Lys yields a protein with a further reduced capacity to bind CCR5, but putting Ala in this position surprisingly has an even larger effect on binding, making it the least able of the

[2] We have previously demonstrated that increasing ionic strength improves the ability of the protein to dimerize (*1*). L34A displays a 5−10-fold weaker dimer affinity than the wild-type protein under low salt conditions, as observed in HSQC spectra (data not shown). However, in the presence of 150 mM NaCl, the difference between L34A and wild-type MIP-1β was difficult to quantitate since the values are near the limit of detection for this method.

mutants to interact with the receptor (see Figure 6 and Table 1). The variation in binding ability of our Phe13 mutants indicates that the aromaticity of Phe13 contributes to its strength of binding. It is interesting to note that most CC chemokines have a Phe or Tyr in this position, whereas the CXC chemokines generally contain a Leu, Ile, or Val at this position. This disparity may partially explain the lack of cross-reactivity between chemokines of one subfamily and receptors of another.

The near loss of the side chain at position 13 (replacement of Phe with Ala) is significantly worse for receptor association than the introduction of additional functional groups into the binding site, indicating a large pocket on the receptor to be filled by the chemokine. Additionally, the necessity of having a Phe or Tyr at position 13 for high activity suggests that the binding pocket on the CCR5 receptor selectively accommodates an aromatic side chain. At the very least, this implies a large flexible hydrophobic pocket in the receptor, and it may also imply the presence of aromatic amino acids on CCR5 that contribute to chemokine binding. Epitope mapping (*47*) and receptor chimeragenesis (*48*, *49*) have shown that the second extracellular loop (ECL2) of CCR5 is the primary determinant in ligand binding. This loop is composed of about 30 residues (168−197), seven of which are aromatic. Indeed, Tyr-184 is located in ECL2 and was shown by Drajic et al. (*50*) to be important for MIP-1β and RANTES binding. In a more recent study, it was found by some of us that both aromatic and charged residues on the CCR5 N-terminus contribute to the binding of chemokines (*51*). Therefore, it is possible that the binding determinants of MIP-1β including Phe13 interact with aromatic residues in CCR5 at either of these two receptor sites.

Why then do the vast majority of CC chemokines form dimers? Possibly chemokine dimerization is simply an artifact of the high concentrations required for structural determination. It is also possible that the dimer may have a role in binding cell surface sugars. Chemokines are known to bind glycosaminoglycans, although the effect of this binding on activity is not well understood. Heparin has been shown to aggregate dimer-forming CC and CXC chemokines but not to aggregate a monomeric variant of IL-8 (*30*). In addition, the presence of heparan sulfate was shown to enhance the anti-HIV activity of RANTES (*31*). An alternative possibility is that an (inactive) chemokine dimer may allow tighter control of local concentrations of (active) chemokine monomer, although the available evidence only points to an active monomer and does not speak to the activity or inactivity of the dimer form.

CONCLUSION

It appears likely that the monomeric form of MIP-1β is responsible for activation of the CCR5 receptor. Our results indicate that the residues preceding the conserved CC motif in MIP-1β are involved in activation of the CCR5 receptor but do not significantly contribute to receptor binding. We have identified the Phe13 position in the so-called N-loop region, as crucial for receptor binding by MIP-1β, and show that mutations at this position can cause a variance of greater than 3 orders of magnitude in the ability of the resultant chemokine to bind the CCR5 receptor. This indicates that amino acids beyond the N-terminus are responsible for receptor binding, in support of the "two-site model".

ACKNOWLEDGMENT

The authors would like to thank Andy LiWang, Frank Delaglio, Sandrine Thieffine, and Chris Jao for their technical assistance.

REFERENCES

1. Laurence, J. S., LiWang, A. C., and LiWang, P. J. (1998) *Biochemistry 37*, 9346−9354.
2. Baggiolini, M., Dewald, B., and Moser, B. (1997) *Annu. Rev. Immunol. 15*, 675−705.
3. Proudfoot, A. E. I. (1998) *Eur. J. Dermatol. 8*, 147−157.
4. Rollins, B. J. (1997) *Blood 90*, 909−928.
5. Cyster, J. C. (1999) *Science 286*, 2098−2102.
6. Rucker, J., and Doms, R. W. (1998) *AIDS Res. Hum. Retroviruses 14*, S241−S246.
7. Baldwin, E. T., Weber, I. T., St. Charles, R., Xuan, J. C., Appella, E., Yamada, M., Matsushima, K., Edwards, B. F., Clore, G. M., Gronenborn, A. M., et al. (1991) *Proc. Natl. Acad. Sci. U.S.A. 88*, 502−506.
8. Chung, C., Cooke, R. M., Proudfoot, A. E. I., and Wells, T. N. C. (1995) *Biochemistry 34*, 3907−9314.
9. Clore, G. M., Appella, E., Yamada, M., Matsushima, K., and Gronenborn, A. M. (1990) *Biochemistry 29*, 1689−1696.
10. Handel, T. M., and Domaille, P. J. (1996) *Biochemistry 35*, 6569−6584.
11. Lodi, P. J., Garrett, D. S., Kuszewski, J., Tsang, M. L., Weatherbee, J. A., Leonard, W. J., Gronenborn, A. M., and Clore, G. M. (1994) *Science 263*, 1762−1767.
12. Lubkowski, J., Bujacz, G., Boque, L., Domaille, P. J., Handel, T. M., and Wlodawer, A. (1997) *Nat. Struct. Biol. 4*, 64−69.
13. Meunier, A., Bernassau, J.-M., Guillemot, J.-C., Ferrara, P., and Darbon, H. (1997) *Biochemistry 36*, 4412−4422.
14. Shao, W., Jerva, F., West, J., Lolis, E., and Schweitzer, B. I. (1998) *Biochemistry 37*, 8303−8313.
15. Skelton, N. J., Aspiras, F., Ogez, J., and Schall, T. J. (1995) *Biochemistry 34*, 5329−5342.
16. Mizoue, L. S., Bazan, J. F., Johnson, E. C., and Handel, T. M. (1999) *Biochemistry 38*, 1402−1414.
17. Gong, J.-H., and Clark-Lewis, I. (1995) *J. Exp. Med. 181*, 631−640.
18. Clark-Lewis, I., Kim, K.-S., Rajarathnam, K., Gong, J.-H., Dewald, B., Moser, B., Baggiolini, M., and Sykes, B. D. (1995) *J. Leukocyte Biol. 57*, 703−711.
19. Gong, J.-H., Uguccioni, M., Dewald, B., Baggiolini, M., and Clark-Lewis, I. (1996) *J. Biol. Chem. 271*, 10521−10527.
20. Pakianathan, D. R., Kuta, E. G., Artis, D. R., Skelton, N. J., and Hébert, C. A. (1997) *Biochemistry 36*, 9642−9648.
21. Weber, M., Uguccioni, M., Baggiolini, M., Clark-Lewis, I., and Dahinden, C. A. (1996) *J. Exp. Med. 183*, 681−685.
22. LiWang, A. C., Cao, J. J., Zheng, H., Lu, Z., Peiper, S. C., and LiWang, P. J. (1999) *Biochemistry 38*, 442−453.
23. Sticht, H., Escher, S. E., Schweimer, K., Forssmann, W.-G., Rosch, P., and Adermann, K. (1999) *Biochemistry 38*, 5995−6002.
24. Crump, M. P., Gong, J. H., Loetscher, P., Rajarathnam, K., Amara, A., Arenzana-Seisdedos, F., Virelizier, J. L., Baggiolini, M., Sykes, B. D., and Clark-Lewis, I. (1997) *EMBO J. 16*, 6996−7007.
25. Rajarathnam, K., Sykes, B. D., Kay, C. M., Dewald, B., Geiser, T., Baggiolini, M., and Clark-Lewis, I. (1994) *Science 264*, 90−92.
26. Leong, S. R., Lowman, H. B., Liu, J., Shire, S., Deforge, L. E., Gillece-Castro, B. L., McDowell, R., and Hébert, C. A. (1997) *Protein Sci. 6*, 609−617.
27. Paolini, J. F., Willard, D., Consler, T., Luther, M., and Krangel, M. S. (1994) *J. Immunol. 153*, 2704−2717.
28. Paavola, C. D., Hemmerich, S., Grunberger, D., Polsky, I., Bloom, A., Freedman, R., Mulkins, M., Bhakta, S., McCarley, D., Wiesent, L., Wong, B., Jarnagin, K., and Handel, T. M. (1998) *J. Biol. Chem. 273*, 33157−33165.
29. Zhang, Y., and Rollins, B. J. (1995) *Mol. Cell. Biol. 15*, 4851−4855.

30. Hoogewerf, A. J., Kuschert, G. S. V., Proudfoot, A. E. I., Borlat, F., Clark-Lewis, I., Power, C. A., and Wells, T. N. C. (1997) *Biochemistry 36*, 13570−13578.
31. Wagner, L., Yang, O. O., Garcia-Zepeda, E. A., Ge, Y., Kalams, S. A., Walker, B. D., Pasternack, M. S., and Luster, A. D. (1998) *Nature 391*, 908−911.
32. Kuna, P., Reddigari, S. R., Schall, T. J., Rucinski, D., Sadick, M., and Kaplan, A. P. (1993) *J. Immunol. 150*, 1932−1943.
33. Blanpain, C., Lee, B., Vakili, J., Doranz, B. J., Govaerts, C., Migeotte, I., Sharron, M., Dupriez, V., Vassart, G., Doms, R. W., and Parmentier, M. (1999) *J. Biol. Chem. 274*, 18902−18908.
34. Wishart, D. S., Bigam, C. G., Yao, J., Abildgaard, F., Dyson, H. J., Oldfield, E., Markley, J. L., and Sykes, B. D. (1995) *J. Biomol. NMR 6*, 135−140.
35. Tjandra, N., Feller, S. E., Pastor, R. W., and Bax, A. (1995) *J. Am. Chem. Soc. 117*, 12562−12566.
36. Farrow, N. A., Muhandiram, R., Singer, A. U., Pascal, S. M., Kay, C. M., Gish, G., Shoelson, S. E., Pawson, T., Forman-Kay, J. D., and Kay, L. E. (1994) *Biochemistry 33*, 5984−6003.
37. Delaglio, F., Gresiek, S., Vuister, G. W., Zhu, G., Pfeifer, J., and Bax, A. (1995) *J. Biomol. NMR 6*, 277−293.
38. Patel, S. R., Evans, S., Dunne, K., Knight, G. C., Morgan, P. J., Varley, P. G., and Craig, S. (1993) *Biochemistry 32*, 5466−5471.
39. Graham, G. J., MacKenzie, J., Lowe, S., Tsang, L.-S., Weatherbee, J. A., Issacson, A., Medicherla, J., Fang, F., Wilkinson, P. C., and Pragnell, I. B. (1994) *J. Biol. Chem. 269*, 4974−4978.
40. Mayo, K. H., and Chen, M.-J. (1989) *Biochemistry 28*, 9469−9478.
41. Kay, L. E., Torchia, D. A., and Bax, A. (1989) *Biochemistry 28*, 8972−8979.
42. Wells, T. N. C., Power, C. A., Lusti-Narasimhan, M., Hoogewerf, A. J., Cooke, R. M., Chung, C., Peitsch, M. C., and Proudfoot, A. E. I. (1996) *J. Leukocyte Biol. 59*, 53−60.
43. Clark-Lewis, I., Schumacher, C., Baggiolini, M., and Moser, B. (1991) *J. Biol. Chem. 266*, 23128−23134.
44. Hébert, C. A., Vitangcol, R. V., and Baker, J. B. (1991) *J. Biol. Chem. 266*, 18989−18994.
45. Lowman, H. B., Slagle, P. H., DeForge, L. E., Wirth, C. M., Gillece-Castro, B. L., Bourell, J. H., and Fairbrother, W. J. (1996) Exchanging interleukin-8 and melanoma growth-stimulating activity receptor binding specificities. *J. Biol. Chem. 271*, 14344−14352.
46. Czaplewski, L. G., McKeating, J., Craven, C. J., Higgins, L. D., Appay, V., Brown, A., Dudgeon, T., Howard, L. A., Meyers, T., Owen, J., Palan, S. R., Tan, P., Wilson, G., Woods, N. R., Heyworth, C. M., Lord, B. I., Brotherton, D., Christison, R., Craig, S., Cribbes, S., Edwards, R. M., Evans, S. J., Gilbert, R., Morgan, P., and Hunter, M. G., et al. (1999) *J. Biol. Chem. 274*, 16077−16084.
47. Lee, B., Sharron, M., Blanpain, C., Doranz, B. J., Vakili, J., Setoh, P., Berg, E., Liu, G., Guy, H. R., Durell, S. R., Parmentier, M., Chang, C. N., Price, K., Tsang, M., and Doms, R. W. (1999) *J. Biol. Chem. 274*, 9617−9626.
48. Samson, M., LaRosa, G., Libert, F., Paindavoine, P., Detheux, M., Vassart, G., and Parmentier, M. (1997) *J. Biol. Chem. 272*, 24934−24941.
49. Wu, L., LaRosa, G., Kassam, N., Gordon, C. J., Heath, H., Ruffing, N., Chen, H., Humblias, J., Samson, M., Parmentier, M., Moore, J. P., and Mackay, C. R. (1997) *J. Exp. Med. 186*, 1373−1381.
50. Drajic, T., Trkola, A., Lin, S., Nagashima, K. A., Kajumo, F., Zhao, L., Olson, W. C., Wu, L., Mackay, C. R., Allaway, G. P., Sakmar, T. P., Moore, J. P., and Maddon, P. J. (1998) *J. Virol. 72*, 279−285.
51. Blanpain, C., Doranz, B. J., Vakili, J., Rucker, J., Govaerts, C., Baik, S. S. W., Lorthioir, O., Migeotte, I., Libert, F., Baleux, F., Vassart, G., Doms, R. W., and Parmentier, M. (1999) *J. Biol. Chem. 274*, 34719−34727.

BI9923196